Title

Development of platforms for functional characterization and production of phenazines using a multi-chassis approach via CRAGE

Authors

Ke, Jing

Zhao, Zhiying

Coates, Cameron R

et al.

Publication Date

2022

DOI

10.1016/j.ymben.2021.11.012

Peer reviewed

Development of platforms for functional characterization and production of phenazines using a multi-chassis approach via CRAGE

Jing Ke[1], Zhiying Zhao[1], Cameron R. Coates[1,2], Michalis Hadjithomas[1], Andrea Kuftin[1], Katherine Louie[1], David Weller [3,4], Linda Thomashow [3,4], Nigel J. Mouncey[1,5], Trent R. Northen [1,5], Yasuo Yoshikuni [1,2,5,6,7#]

[1] US Department of Energy Joint Genome Institute, Lawrence Berkeley National Laboratory, Berkeley, CA, USA

[2] Biological Systems and Engineering Division, Lawrence Berkeley National Laboratory, Berkeley, CA, USA

[3] USDA Agricultural Research Service, Wheat Health, Genetics and Quality, Washington State University, Pullman, WA, USA

[4] Department of Plant Pathology, Washington State University, Pullman, WA, USA

[5] Environmental Genomics and Systems Biology Division, Lawrence Berkeley National Laboratory, Berkeley, CA, USA

[6] Center for Advanced Bioenergy and Bioproducts Innovation, Lawrence Berkeley National Laboratory, Berkeley, California 94720, USA

[7] Global Center for Food, Land, and Water Resources, Hokkaido University, Hokkaido, 060-8589, Japan

#Correspondence: yyoshikuni@lbl.gov

Abstract

Phenazines (Phzs), a family of chemicals with a phenazine backbone, are secondary metabolites with diverse properties such as antibacterial, anti-fungal, or anticancer activity. The core derivatives of phenazine, phenazine-1-carboxylic acid (PCA) and phenazine-1,6-dicarboxylic acid (PDC), are themselves precursors for various other derivatives. Recent advances in genome mining tools have enabled researchers to identify many biosynthetic gene clusters (BGCs) that might produce novel Phzs. To characterize the function of these BGCs efficiently, we performed modular construct assembly and subsequent multi-chassis heterologous expression using chassis-independent recombinase-assisted genome engineering (CRAGE). CRAGE allowed rapid integration of a PCA BGC into 23 diverse γ-proteobacteria species and allowed us to identify top PCA producers. We then used the top five chassis hosts to express four partially refactored PDC BGCs. A few of these platforms produced high levels of PDC. Specifically, *Xenorhabdus doucetiae* and *Pseudomonas simiae* produced PDC at a titer of 293 mg/L and 373 mg/L, respectively, in minimal media. These titers are significantly higher than those previously reported. Furthermore, selectivity toward PDC production over PCA production was improved by up to 9-fold. The results show that these strains are promising chassis for production of PCA, PDC, and their derivatives, as well as for function characterization of Phz BGCs identified via bioinformatics mining.

Graphical abstract

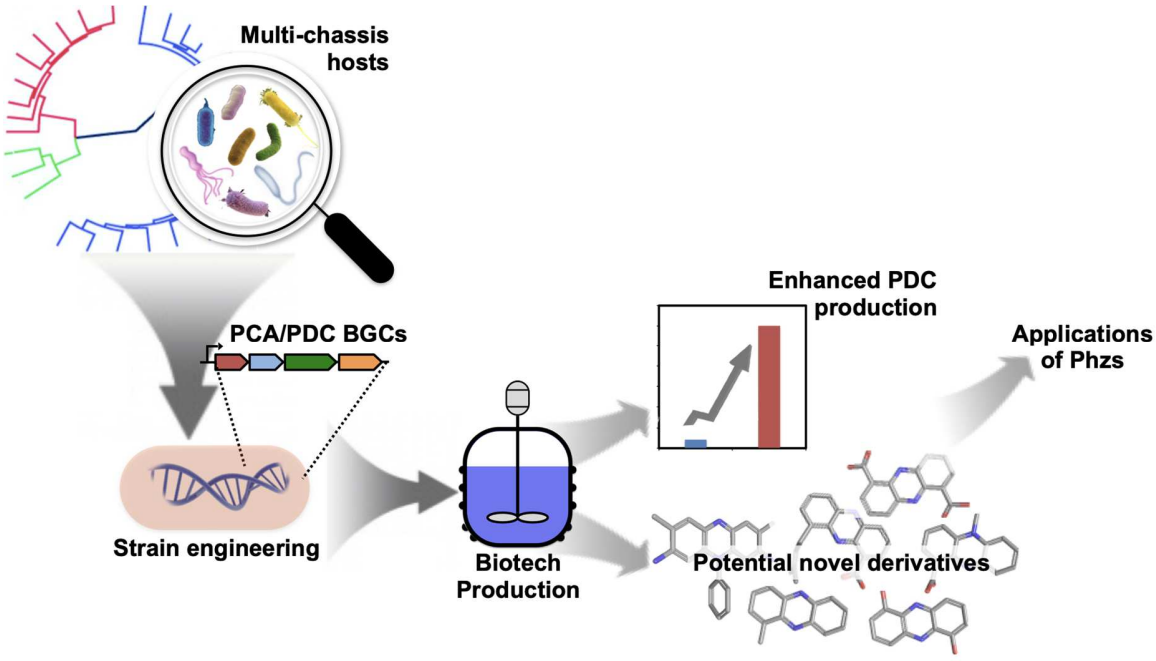

1. Introduction

Phenazines (Phzs), a family of heterocyclic, nitrogen-containing chemicals with a phenazine backbone, are good candidates for many clinical and agricultural applications. Produced by soil and marine bacteria, these secondary metabolites (also known as specialized metabolites or natural products) often have antibacterial, anti-fungal, anti-tumor, anti-malarial, or anti-parasitic activity (Laursen and Nielsen, 2004). For example, some Phzs benefit plant growth and crop production. Phenazine-1-carboxylic acid (PCA) is registered and commercially used as a highly efficient and environmentally friendly natural fungicide in China to improve crop production. Phzs can also shuttle electrons efficiently via reversible oxidation and reduction (Pierson and Pierson, 2010). This electron movement facilitates anaerobic respiration and electrochemical reduction of minerals such as inorganic phosphate and iron, making them, as well as organic compounds associated with mineral phases, more available to plants (Hernandez et al., 2004). Metabolic engineering is a promising approach

to delivering strains that can produce large quantities of useful Phzs and serve as platforms for discovering new bioactive Phz derivatives.

Phz biosynthesis involves chorismic acid produced via the shikimate pathway, with two molecules of the chorismate-derived monomeric precursor pairing head-to-tail to form the basic Phz scaffold (McDonald et al., 2001). Sequential modifications on the functional group lead to Phzs with various biological activities (McDonald et al., 2001; Baron et al., 1989). Phz pathways have been identified in various lineages of bacteria, primarily *Proteobacteria* (e.g., *Pseudomonas* and *Pelagibacter*) and *Actinobacteria* (e.g., *Streptomyces*) (Mavrodi et al., 2010). Among these pathways, a core *phz* biosynthetic gene cluster (BGC) comprising *phzA–G* genes is conserved (Mavrodi et al., 2010). This BGC is responsible for the synthesis of PCA and phenazine-1,6-dicarboxylic acid (PDC), which are the precursors for all other Phzs (Blankenfeldt and Parsons, 2014; Pierson and Pierson, 2010; Abraham et al., 2015) (Figure 1). Accessory enzymes can further diversify Phz secondary metabolites, (Laursen and Nielsen, 2004; Mentel et al., 2009; Guttenberger et al., 2017; Bauman et al., 2019). We, as well as others, have demonstrated that synthetic biology is a promising approach (Coates, et al., 2018; Smanski et al., 2016; Kunakom and Eustáquio, 2019). Expression of unique accessory modular Phz-modifying enzymes along with the core PCA BGC will further enable exploration of a wide variety of Phz structures and pathways (Coates et al., 2018).

In the present study, our goal was to develop a strain that could produce high levels of PDC and serve as a host for discovery and production of PDC derivatives. PDC, which has better antibacterial activity than PCA, could potentially be developed as an antibacterial biopesticide (Dasgupta et al., 2015). PDC shows potentially substantial cytotoxicity against both Gram-positive and Gram-negative bacteria (Dasgupta et al., 2015). In addition, PDC forms an array of derivatives (Figure 1) with high activity, including iodinin (anticancer) (Podojil and Gerber, 1967; Myhren et al., 2013), lomofungin (antibacterial and antifungal)

(Johnson and Dietz, 1969; Zhang et al., 2015), esmeraldins (antimicrobial and antitumor) (Rui et al., 2012), saphenamycin (antimicrobial) (Geiger et al., 1988), the broad-spectrum antibiotic D-alanyl-griseoluteic acid (Giddens et al. 2002), and myxin (antimicrobial and cytotoxic) (Zhao et al., 2016). With the advent of genome sequencing and bioinformatics capabilities, the ability to search for BGCs with unknown function has dramatically improved. The fact that new Phz secondary metabolites are continually discovered in nature implies that a large reservoir of undiscovered metabolites with biological significance likely exists. Our colleagues at the Joint Genome Institute have developed a database called Integrated Microbial Genomes and Microbiomes - Atlas of Biosynthetic Gene Clusters (IMG-ABC) (Hadjithomas et al., 2015). Using this database of more than 25,000 isolated genomes, we identified over 1,000 putative Phz BGCs, including 26 with unique pathway architectures that were previously uncharacterized.

Despite PDC's potential to generate more complex and bioactive Phz derivatives than PCA can, understanding of PDC biosynthesis is limited, while biosynthesis of PCA by *Pseudomonas* sp. has been studied extensively, and a strain has been engineered that can produce high levels (~10 g/L) of PCA (Jin et al., 2015). The activity of the enzymes PhzA/B and PhzG may be important for distinguishing the PDC pathway from the PCA pathway (Xu et al., 2013; Blankenfeldt et al., 2013); while PDC production depends on flavin-dependent oxidations of its intermediate catalyzed by PhzG, PCA is produced when the intermediate undergoes spontaneous oxidative decarboxylation. In addition, it has been demonstrated that PhzA is a shunt switch for PDC biosynthesis (Guo et al., 2017). Although efforts are still limited, metabolic engineering for PDC production has also been explored. For example, Rui et al. (2012) obtained PDC production (~7 mg/L) in *Escherichia coli* by expression of PhzCDEF from *Pseudomonas synxantha* 2-79 with EsmA1 (PhzA/B homolog) and EsmA2 (PhzG homolog) from *Streptomyces antibioticus*. In other approaches, Guo et al. (2020) replaced PhzG in *P. chlororaphis* GP72 with its homolog derived from *S. lomondensis*, increasing PDC production to ~50 mg/L. Further, point mutations to

the *phzA* gene in *P. chlororaphis* HT66 led to PDC production of ~100 mg/L (Guo et al., 2017). In all cases, however, more PCA has been formed than PDC (1- to 2-fold more PCA than PDC production). For production of PDC with higher selectivity, we expected that both selectivity and activity of PhzA/B and PhzG for PDC would need to be optimal and well balanced. To develop PDC pathways with higher selectivity and activity, we combined the approaches of Rui et al. (discussed above) and genome mining through IMG-ABC.

We first investigated PCA production, using our recently developed technology. Called "chassis-independent recombinase-assisted genome engineering" (CRAGE), this technology enables single-step integration of complex BGC constructs directly into genomes of diverse microbial species and subsequent expression after a landing pad is integrated (Figure 2A) (Wang et al., 2019, Ke and Yoshikuni, 2020, Wang et al., 2020). We had previously used CRAGE to express 10 natural-product BGCs from *Photorhabdus luminescens* in over 20 different γ-proteobacteria species (Wang et al., 2019). We had selected this panel of strains based on availability of their genome sequences and to cover a broad range of genetic identity to the native BGC strain as indicated by 16S rRNA sequences (with all selected strains showing greater than 80% identity). In this previous work, the multi-chassis approach provided significant advantages for BGC activation. It allowed us to activate ~6 BGCs and alter each BGC's ability to selectively produce a given secondary metabolite product. Using a range of bacteria as heterologous chassis strains, the multi-chassis approach harnessed naturally occurring physiological diversity (e.g., relaxation of regulatory controls, enhanced substrate availability, and resistance to product toxicity) and enabled efficient development of platform strains for the expression and function characterization of BGCs (Wang et al., 2019).

Because of the success of this previous work, we thought that the multi-chassis approach might allow us to identify chassis strains better suited to PDC production than those previously explored, and that it would be logical to use a

similar panel as a first step toward demonstrating the utility of this strategy (Zhang et al., 2016). For the present study, therefore, we used CRAGE to explore the ability of a similar panel, 23 different γ-proteobacteria species across 11 different genera, to produce PCA (Figure 2B). We selected the top five heterologous PCA producers for expression of four partially refactored PDC BGCs (Figure 2B) and identified a few chassis strains suitable for production of PDC.

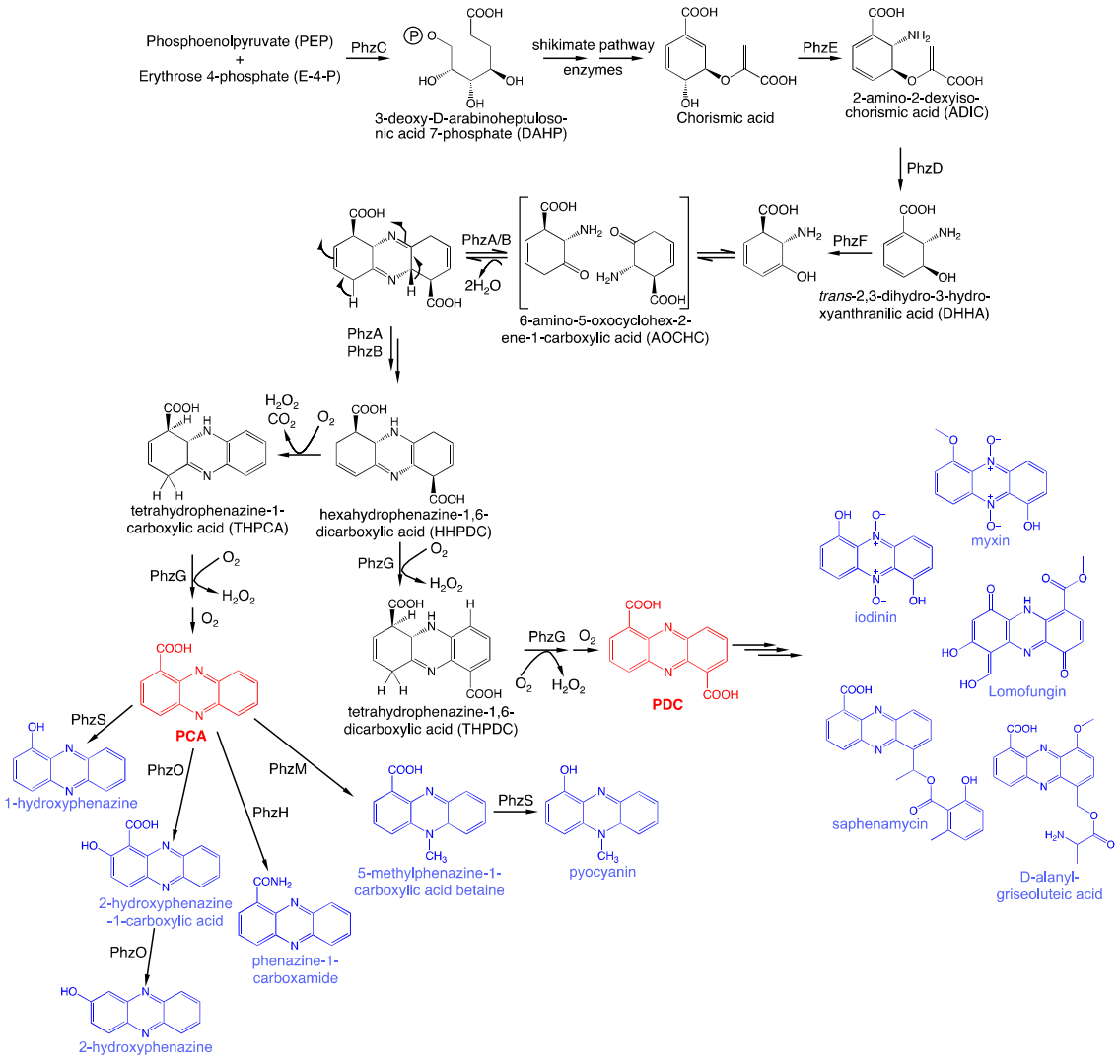

Figure 1. Current understanding of the core Phzs (PCA and PDC) biosynthetic pathways. The core Phz biosynthetic locus (*phzA–G*) is highly conserved among Phz-producing strains of *Pseudomonas* spp (Gross and Loper, 2009; Schneemann et al.,

2011; Blankenfeldt and Parsons, 2014). PhzC encodes a 3-deoxy-d-arabino-heptulosonate-7-phosphate (DAHP) synthase, which catalyzes the first step of the shikimate pathway to redirect intermediates from primary metabolism into Phz biosynthesis. Chorismic acid is converted to 2-amino-4-deoxychorismic acid (ADIC) catalyzed by the anthranilate synthase homolog PhzE (McDonald et al., 2001). The isochorismatase PhzD cleaves ADIC to generate trans-2,3-dihydro-3-hydroxyanthranilic acid (DHHA) (Parsons et al., 2003). The isomerase PhzF initiates a 1,5-prototropic shift, yielding an enol that converts to 6-amino-5-oxocyclohex-2-ene-1-carboxylic acid (AOCHC) (Blankenfeldt et al., 2004), two molecules of which subsequently undergo a symmetrical head-to-tail double condensation for a double imine spontaneously, catalyzed by the dimeric protein PhzA/B *in vivo*. Together, PhzA and its highly homologous copy PhzB form a dimeric protein of the Δ5-3-ketosteroid isomerase/nuclear transport factor 2 family, which catalyzes a reaction that orients two substrate molecules and neutralizes the negative charge of tetrahedral intermediates through protonation. Possibly catalyzed by PhzA/B, the condensation product rearranges further to form hexahydrophenazine-1,6-dicarboxylic acid (HHPDC) (to prevent back-hydrolysis), which is prone to oxidation and undergoes oxidative decarboxylation to generate tetrahydrophenazine-1-carboxylic acid (THPCA) without enzymatic catalysis. Competing with the spontaneous reaction to form THPCA, the FMN-dependent oxidase PhzG converts HHPDC to tetrahydrophenazine-1,6-dicarboxylic acid (THPDC). The final aromatization of the ring system of THPCA or THPDC is performed by PhzG, leading to PCA or PDC (Parsons et al., 2004a). Finally, the PCA or PDC precursors can be converted to various PCA or PDC derivatives by strain-specific Phz enzymes.

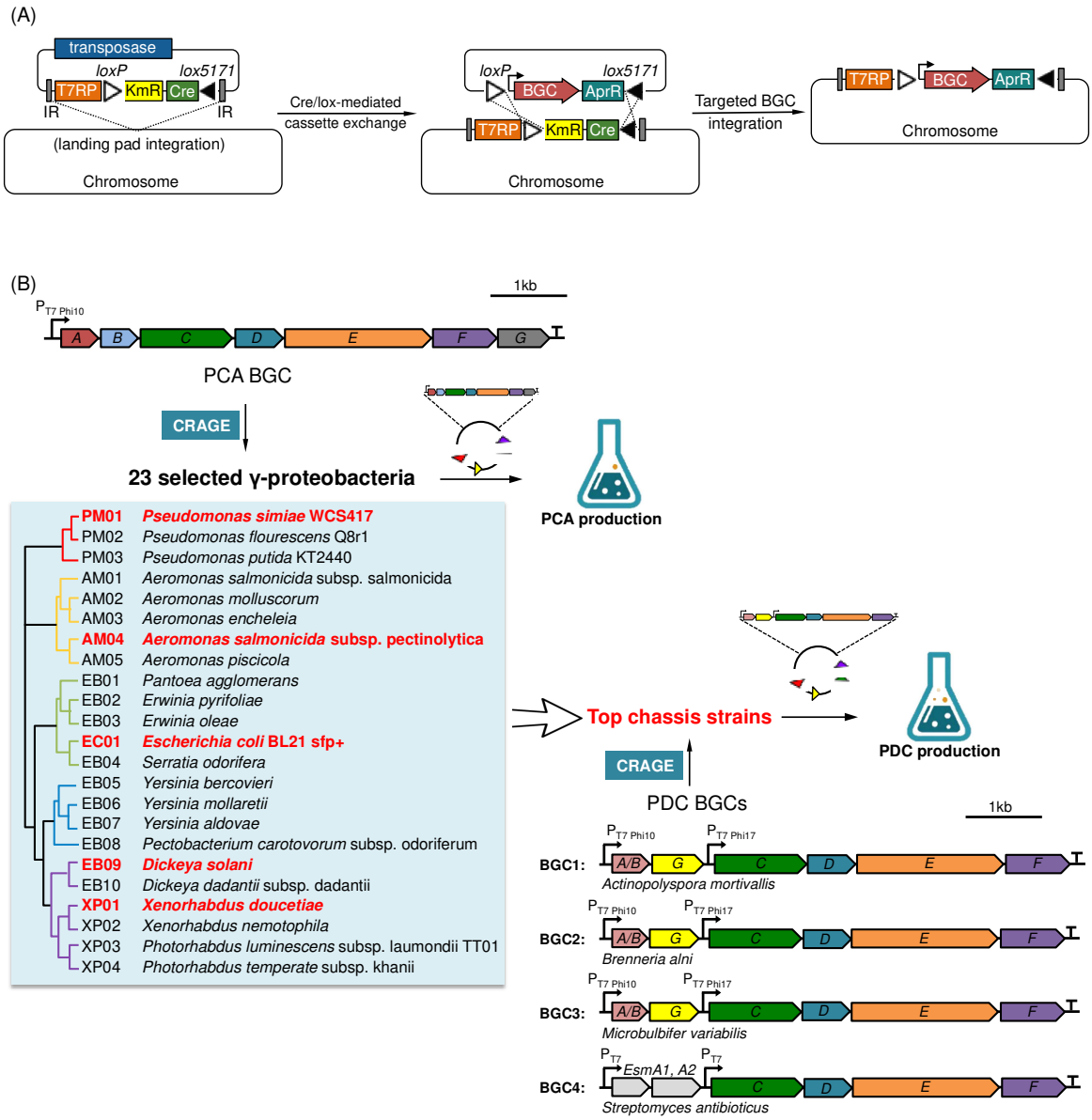

Figure 2. Activation of a partially refactored PDC BGC using a multi-chassis approach enabled by CRAGE. (A) Scheme for CRAGE technology. First, a transposon containing a landing pad (LP) is integrated into the genome of the recipient cell. The LP contains a *Cre* recombinase gene flanked by mutually exclusive lox sites. Then, flanked by the same lox sites, the genes of interest are integrated into the LP on the recipient chromosome, catalyzed by Cre recombinase. (B) Multi-chassis engineering in this study for optimized expression of Phz BGCs. Modular and multi-chassis approaches were used to integrate a PCA BGC into 23 diverse γ-proteobacteria species. The top five PCA producers were subsequently selected for expression of four partially refactored PDC

BGCs. For BGC4, EsmA1 and EsmA2 originated from *Streptomyces antibioticus* Tü 2706; these are homologs equivalent to PhzA/B and PhzG, respectively, which have been reported to significantly promote PDC production (Rui et al., 2012).

2. Materials and Methods

2.1. Microbial strains and reagents

All chemical reagents were purchased from MilliporeSigma unless otherwise stated. *E. coli* Top10 or EC100D pir+ strains were used for plasmid construction. *E. coli* BW29427 was used for conjugal transformation. The chassis bacterial strains used for PCA and PDC production in this study are listed in Table 1.

Table 1. Strains containing CRAGE landing pad.

Strain #	Strain name	Screening Kanamycin (μg/mL)	Screening Apramycin (μg/mL)
PM01	*Pseudomonas simiae WCS417*	200	50
PM02	*Pseudomonas fluorescens Q8r1*	200	50
PM03	*Pseudomonas putida KT2440*	500	150
AM01	*Aeromonas salmonicida salmonicida*	50	50
AM02	*Aeromonas molluscorum*	200	150
AM03	*Aeromonas encheleia*	200	100
AM04	*Aeromonas salmonicida pectinolytica*	200	150
AM05	*Aeromonas piscicola*	200	150
EB01	*Pantoea agglomerans*	50	100
EB02	*Erwinia pyrifoliae*	50	50
EB03	*Erwinia oleae*	50	50
EC01	*E. coli BL21 sfp+*	50	50
EB04	*Serratia odorifera*	200	100
EB05	*Yersinia bercovieri*	50	200
EB06	*Yersinia mollaretii*	200	150
EB07	*Yersinia aldovae*	50	150
EB08	*Pectobacterium carotovorum odoriferum*	50	50
EB09	*Dickeya solani*	50	50
EB10	*Dickeya dadantii dadantii*	50	50
XP01	*Xenorhabdus doucetiae*	50	100
XP02	*Xenorhabdus nematophila*	50	50

XP03	*Photorhabdus luminescens laumondii TT01*	50	100
XP04	*Photorhabdus temperata khanii*	50	100

2.2. Genome mining to find appropriate phzA/B and phzG for PDC BGCs

As Hadjithomas et al. (2015) described, a global survey of BGCs containing at least six of the seven core Phz biosynthesis genes (Mavrodi et al., 1998) was conducted against the full complement of 25,000+ isolate genomes within the Integrated Microbial Genomes and Microbiomes - Atlas of Biosynthetic Gene Clusters (IMG-ABC) (https://img.jgi.doe.gov/abc). IMG-ABC is an atlas database of BGCs and the chemicals they are known to produce, made possible through the integration of the Atlas of Biosynthetic Gene Clusters with the Integrated Microbial Genomes and Microbiomes (IMG) data system (Markowitz et al., 2014a, b). To be specific, we first identified BGCs using ClusterFinder (Cimermancic et al., 2014) for all isolate genomes and metagenomes in IMG and IMG/M, respectively. ClusterFinder predicts putative BGCs based on the Pfam functional annotation of genes available in the integrated context within IMG.

Candidate genome data sets were integrated into IMG and automatically processed through IMG's BGC prediction pipeline, constantly feeding IMG-ABC with new putative BGCs to provide the knowledge base needed for heterologous expression of Phz BGCs that potentially produce PDC compounds. BGCs were predicted in isolate genomes by the type of biosynthetic enzymes they contain via antiSMASH (version 2.2) (Blin et al., 2013). BGC predictions were filtered to eliminate BGCs that contained fewer than six of the essential Phz genes, with a predicted probability of less than 0.3. Additionally, BGC content was analyzed to identify Pfam categories that are not known to be associated with secondary metabolism but that are present as positive training features within ClusterFinder. These included Pfam categories such as prophage proteins (PF04883, PF05709, and PF06199), protein secretion systems (PF08817, PF10140, and PF10661), inorganic ion transport proteins (PF02421 and PF11604), and families

representing DNA/RNA polymerases, whose presence leads to false-positive BGC predictions (Hadjithomas et al., 2015).

2.3. Construction of Phz BGCs for PCA and PDC production

For PCA BGC constructs, we used a pW5_PCA plasmid we had previously built (Coates et al., 2018). This plasmid contains the *P. synxantha* 2-79 *phz* operon comprising *phzA–G* genes under the control of a T7 promoter (pW5_PCA).

For PDC BGC4 constructs, we amplified *EsmA1* and *EsmA2* genes from the pSET_EsmA1_A2 plasmid (from Dr. Rui, Louisiana State University) and assembled them, along with *phzC–F*, into an accessory vector, pApr_2L (R6K ori), via Gibson Assembly (Gibson et al., 2009) to yield pApr_SaPDC. This plasmid was confirmed by sequencing. Then modules were refactored and synthesized, and, along with *phzC-F*, the *phzA/B* and *phzG* homolog genes *EsmA1* and *EsmA2* were assembled to build pApr_AmPDC2 (BGC1), pApr_MvPDC2 (BGC2), and pApr_BaPDC2 (BGC3). The modules were designed using BOOST (Build-Optimization Software Tools) (Oberortner et al., 2017). Fusion PCRs and Gibson Assembly were employed to assemble three *phzA/B* and *phzG* strings into an accessory vector, pApr_2L. Construction of pApr_PDC2 variants was confirmed by sequencing. The plasmid DNA of PDC variants in the pApr_2L accessory vector was transformed into competent cells of *E. coli* BW29427 containing pW5BB2LKmLacICre, and 0.1mM IPTG was used to induce Cre expression. Positive clones with successful replacement of kanamycin with PDC_Apramycin modules via Cre-lox recombination were selected. All primers used to assemble PDC constructs are listed in Supplementary Table 2. The full sequences and maps of all constructs are available in GenBank format as supplementary material.

2.4. Chromosomal integration of PCA and PDC BGCs into diverse chassis strains via CRAGE

A PCA (or PDC) BGC was integrated into each of 23 chassis strains (or into the top five PCA producers) (Table 1) via CRAGE (Wang et al., 2019). Conjugation donor strains were *E. coli* BW29427 (also known as *E. coli* WM3064) containing pW5_PCA or pW5_PDC2 variants. Recipient strains were the 23 γ-proteobacteria making up the chassis strain panel (Table 1) (Wang et al., 2019). Conjugation was performed using a previously reported method (Wang et al., 2019). The conjugated recipient bacteria were streaked on LB plates with appropriate concentrations of apramycin. Colonies were tested for kanamycin sensitivity to determine whether the landing pads (LPs) were successfully replaced with PCA or PDC BGCs (Table 1 shows corresponding antibiotic selection concentrations for each strain). Four PDC BGC variants were conjugated to the top five PCA producers.

2.5. Production of PCA and PDC

Strains harboring the PCA BGCs were streaked on LB agar plates containing 50 μg/mL apramycin (Apr50) and were incubated at 28 °C for 24 hr. A single colony was inoculated into liquid LB medium containing Apr50, and the culture was grown overnight. For pre-screening [Figure 3A and 3C]), an aliquot of the LB culture was inoculated into 25 mL of fresh M9-based medium (4 g/L glucose, 5 g/L yeast extract, 1X M9 salts, 0.24 g/L $MgSO_4$, 11.1 mg/L $CaCl_2$, 3 g/L citric acid monohydrate, 2.5 mL/L trace mineral solution, and 2.5 mL/L vitamin supplement) containing Apr50 in 125 mL flasks to final OD600 of 0.1. This culture was aliquoted to 4 x 5 mL in 50 mL glass tubes, incubated for 5 hours, and then induced with IPTG at final concentrations of 0, 0.01, 0.1 and 1.0 mM, respectively. For PCA reproduction from the top five PCA producers [Figure 3B] and PDC production [Figure 5], an aliquot of the LB culture was inoculated into 5 mL of fresh M9-based medium with Apr50 in 50 mL glass tubes, in triplicates, to final OD600 of 0.1, incubated for 5 hours, and induced with IPTG at the optimal concentration of 0.1 mM for each host strain.

2.6. Extraction of PCA and PDC

To extract PCA and PDC from cultures, 100 µL of culture was first acidified with 100 µL of 1.25% trifluoroacetic acid and then extracted with 1 mL of ethyl acetate. The mixture was then vortexed at 1,500 rpm for 5 min and centrifuged at 3,200 rpm for 5 min. 100 µL of ethyl acetate in the upper phase was removed from each extract and dried at 35 °C in a speed vacuum. The extract was then suspended in 1,000 µL acetonitrile with 1 µg/mL internal standard of 2-amino-3-bromo-5-methylbenzoic acid (ABMBA), 150 µL of which was run through a 0.2-µm filter for liquid chromatography-high resolution mass spectrometry (LC-HRMS) quantification.

2.7. Preparation of authentic standards of Phzs

PCA (Santa Cruz Biotechnology, Inc.) standards were prepared as solutions or suspensions at concentrations of 0, 1, 10, 50, 100, 500, 1,000, and 3,000 mg/L. PDC (Santa Cruz Biotechnology, Inc.) solutions or suspensions were prepared at concentrations of 0, 1, 10, 50, 100, 500, and 1,000 mg/L. Standards of the other Phzs, which were phenazine (TCI America Research Chemicals), pyocyanin (Cayman Chemical Company), and phenazine-1-carboxamide (Cayman Chemical Company), were prepared at concentrations of 10 and 50 mg/L. The extraction procedures are described in section 2.6.

2.8. LC-HRMS analysis

LC-HRMS analysis was performed using an Agilent UHPLC coupled to a Thermo QExactive or QExactive HF (Thermo Scientific, San Jose, CA). Reverse phase chromatography was performed by injecting 2 µL of each sample onto a C18 column (Agilent ZORBAX Eclipse Plus C18, 2.1 x 50 mm, 1.8 µm) held at 60 °C. Chromatography was performed at a flow rate of 0.4 mL/min, with the C18 column equilibrated with 100% buffer A (100% LC-MS water with 0.1% formic acid) for 1 minute, diluting buffer A down to 0% with buffer B (100% ACN with 0.1% formic acid) over an 8-min linear gradient, followed by 1.5 min of isocratic

elution with 100% B. Spectra were collected in positive ion mode, with full MS spectra acquired ranging from 80 to 1,200 *m/z* at 60 k or 70 k resolution, and MS/MS fragmentation data acquired using an average of stepped collision energies of 10, 20, and 40 eV at 17,500 k resolution. Orbitrap instrument parameters included a sheath gas flow rate of 50 (au), an auxiliary gas flow rate of 20 (au), a sweep gas flow rate of 2 (au), a spray voltage of 3 kV, and a capillary temperature of 400 °C.

3. Results

3.1. Multi-chassis approach identified efficient PCA producers

Parallel expression of the PCA BGC across diverse hosts allowed identification of strains favorable for PCA production. CRAGE was used to integrate the PCA BGC into chromosomes of a panel of 23 γ-proteobacteria strains. These strains, together with the control construct, which contained only the LP, were cultivated at four different isopropyl-β-D-thiogalactoside (IPTG) concentrations (0–1 mM). PCA production from each strain was subsequently measured by ultra-performance LC-HRMS. No PCA production was detected in the control strains carrying only the LP. All chassis strains carrying the PCA BGC produced PCA, but at various levels (Figure 3A). The difference between the lowest and the highest producers was as much as 51-fold at the optimal IPTG induction concentration, suggesting that the multi-chassis approach is effective for identifying chassis most suitable for PCA production, among those tested.

Of the four concentrations of IPTG, 0.1 mM was the optimal induction dose for PCA production in all chassis strains except *Yersinia mollaretii* (EB06) and *Erwinia pyrifoliae* (EB02), which produced higher levels of PCA at 0.01 mM. No significant difference among the four IPTG concentrations was detected for *Pseudomonas simiae* WCS417 (PM01), indicating that BGC expression is unlikely the rate-limiting step for this strain and that the strain can be further improved for PCA production.

Among the 23 γ-proteobacteria, *Xenorhabdus doucetiae* (XP01), *E. coli* BL21 (EC01), *P. simiae* WCS417 (PM01), *Aeromonas salmonicida* subsp. pectinolytica (AM04), and *Dickeya solani* (EB09) were identified as the top five chassis strains for PCA production. Then the PCA production experiment was repeated in the top five recombinants in triplicate (Figure 3B) at 0.1 mM IPTG induction, which had been identified as their optimal IPTG concentration for PCA production. The results confirmed XP01_PCA as the strongest PCA producer, with a 131 mg/L production titer in culture, more than 2 times higher than that of the second strongest producer, EC01_PCA. Although PM01 showed the closest phylogenetic similarity to the PCA BGC origin strain of *P. synxantha* 2-79, PM01_PCA produced only around one-third as much PCA as did XP01_PCA. These results demonstrate the power of the purpose-engineered multi-chassis approach enabled by CRAGE for this Phz pathway.

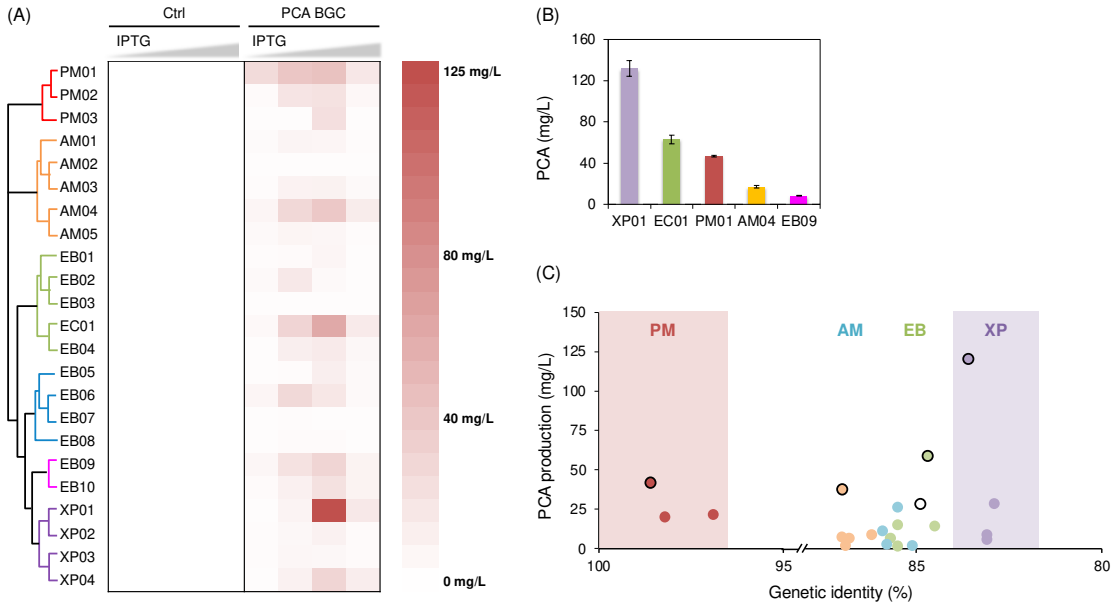

Figure 3. Expression of Phz BGCs in a panel of phylogenetically diverse chassis strains for PCA production. (A) Measured PCA production from the panel of phylogenetically diverse chassis strains induced with different IPTG concentrations (0, 0.01, 0.1, and 1 mM). Heatmap data are presented in Supplementary Table 3. (B) Repeat of PCA production from the top five producers (XP01, EC01, PM01, AM04, and EB09), each induced with 0.1 mM IPTG. Error bars represent s.d.; n = 3 technically independent experiments. (C) Genetic identity of the phylogenetically diverse chassis strains to the PCA BGC origin strain *P. synxantha 2-79* vs. PCA productivity. Each dot

represents a strain and is color-coordinated in the same way as is the phylogenetic tree in Figure 3A. The dots for the top five PCA producers are circled with black. PM: *Pseudomonadales,* AM: *Alteromonadales,* EB: *Enterobacterales*, and XP: *Xenorhabdus* and *Photorhabdus sp.* (*Enterobacterales*).

3.2. BGC:chassis compatibility may be affected by evolutionary distance

Our previous study suggested that BGCs were more efficiently expressed in chassis strains more closely related to the native BGC strains (Wang et al., 2019). We interpreted this to mean that the closely related strains have physiology similar to that of the native BGC strains and can support functional expression of the heterologously introduced BGCs, while regulatory restrictions uniquely associated with the BGCs in their native strains are no longer conserved in the closely related strains. To investigate the relationships between PCA production and genetic distance between chassis and native BGC strains, the highest PCA production of each chassis strain was plotted against the degree of genetic identity (based on 16S rRNA gene sequence) to the native producer, *Pseudomonas synxantha* 2-79 (Figure 3C). We found no obvious correlation between PCA yields and phylogenetic distance between chassis and native strain (Figure 3C). Instead, we found a high producer from each group (PM: *Pseudomonadales,* AM: *Alteromonadales,* EB: *Enterobacterales*, and XP: *Xenorhabdus* and *Photorhabdus sp.* [*Enterobacterales*]). XP01, one of the phylogenetically furthest species from *P. synxantha* 2-79, showed the highest PCA production. This result suggests that the PCA BGC pathway is not highly regulated and that PCA production may instead be limited by the availability of precursors or by the flux through the shikimate pathway rather than by regulatory mechanisms associated with the PCA BGC in *P. synxantha* 2-79. In fact, it is understood that the PCA pathway in *P. synxantha* 2-79 is regulated only by quorum sensing molecules (Khan et al., 2005).

3.3. Genome mining for appropriate phzA/B and phzG for PDC BGCs

To mine *phzA/B* and *phzG* for PDC BGCs, we conducted a global survey of BGCs containing at least six of the seven genes essential for Phz biosynthesis (identified by Mavrodi et al., 1998) against the full complement of 25,000+ genomes within IMG-ABC (which was described by Hadjithomas et al., 2015). Guided by the observations of Rui et al. (2012), we initially selected BGCs that exhibited *phzA/B* and *phzG* homologs and similarities to griseoluteic-acid-producing pathways for investigation of PDC production. Among the 26 pathways filtered from an initial set of 1,000 hits, one pathway came from a marine bacterium (*Microbulbifer variabilis* ATCC 700307) that had been described as able to produce the griseoluteic-acid-derived pelagiomicins (Imamura et al., 1997). The composition of the Phz pathway found in *M. variabilis* was similar to the pathway of the griseoluteic-acid-producing strains of *Pantoea agglomerans* Eh1087 and *Photobacterium halotolerans* DSM 18316 (Giddens et al., 2002; Shi et al., 2019) (Figure 4). Additionally, the Phz pathway found in *Actinopolyspora mortivalis* DSM 44261 exhibited the same griseoluteic acid biosynthesis genes, but in a somewhat different pathway architecture. Therefore, we hypothesized that the *phzA/B* and *phzG* homologs were responsible for PDC biosynthesis in these pathways. Similarly, *Brenneria alni* DSM11811 had those same *phzA/B* and *phzG* homologs, as well as three of the seven genes thought to be responsible for griseoluteic acid biosynthesis (Figure 4). *PhzA* and *phzG* homologs from the Phz pathways in *A. mortivallis* DMS 44261, *M. variabilis* ATCC 700307, and *B. alni* DSM 11811 were identified by Pfam annotations provided in IMG-ABC.

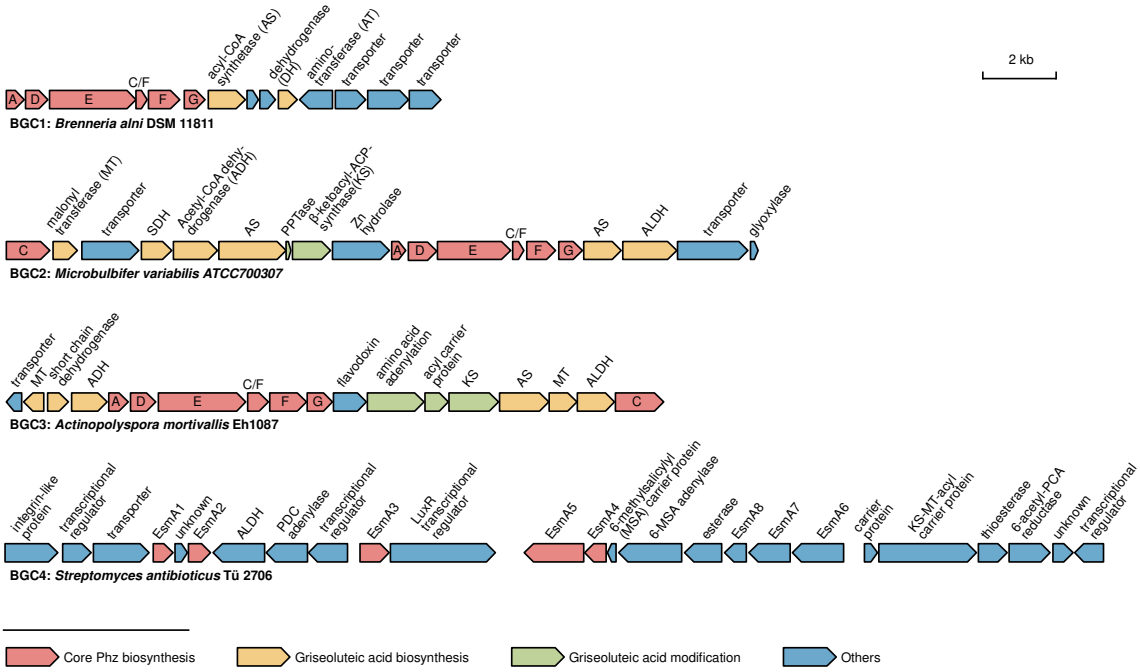

Figure 4. Four native PDC-based Phz BGCs, from *A. mortivallis* DMS 44261, *M. variabilis* ATCC 700307, *B. alni* DSM 11811, and *Streptomyces antibioticus* Tü 2706. BGCs 1–3 were predicted to be capable of producing PDC-based Phzs. For BGC4, EsmA1 was identified for 6-amino-5-oxocyclohex-2-ene-1-carboxylic acid (AOCHC) dimerization and EsmA2 for PDC formation; EsmA3 is DHHA isomerase, EsmA4 is DHHA synthase, EsmA5 is ADIC synthase, EsmA6 is DAHP synthase, EsmA7 is chorismate synthase, and EsmA8 is shikimate kinase.

3.4. Expression of PDC BGCs produced PCA and PDC at various levels

The top five PCA-producing chassis strains (XP01, EC01, PM01, AM04, and EB09) were selected for integration of four PDC BGCs (BGCs 1–4) (Figure 5). The only BGC successfully integrated with EB09 was BGC1. Rui et al. (2012) reported that BGC4 promoted PDC production in *E. coli* when *phzA, B,* and *G* of the PCA BGC were replaced with *EsmA1* (*phzA/B*) and *EsmA2* (*phzG*). Rui et al. demonstrated production of PCA and PDC at ~11.2 mg/L (50 nmol/mL) and ~6.7 mg/L (25 nmol/mL), respectively. We, also, detected a comparable level of PCA and PDC production in EC01_BGC4 (3.9 mg PCA/L and 3 mg PDC/L), and the production levels were higher than those of the other chassis strains.

Notably, expression of BGC1 in PM01 and BGCs 1–3 in XP01 significantly promoted heterologous production of PDC, while relatively mild enhancement was seen in *E. coli*. Expression of only BGC1 led to high PDC production in chassis PM01, which was also the highest PDC producer among all the PDC recombinants we tested, reaching 373 mg/L in culture. Although BGC1 expression and PDC production were weaker in XP01 (268 mg/L) than in PM01, XP01 was most compatible with BGC2 and BGC3, with PDC levels of 242 and 293 mg/L, respectively, which were (respectively) 129-fold and 1,265-fold higher than those of PM01. Among the four PDC BGCs we tested, the γ-proteobacteria chassis hosts showed poorer compatibility with *Streptomyces*-origin BGC4 than with BGCs 1–3.

Presence of PDC pathways in XP01, EC01, and PM01 also increased production of the byproduct PCA accordingly, indicating BGCs 1–4 have promiscuous activity for PCA production. In Rui's results, expression in *E. coli* of the construct similar to our PDC_BGC4 led to higher production titer of PCA than PDC, with a PDC/PCA ratio of 0.5. We had similar results, with BGC4 expression yielding a PDC/PCA ratio of 0.8. Interestingly, PDC and PCA were produced at different ratios depending on the chassis strain (down to a PDC/PCA ratio of 0.2) (Figure 5D), suggesting that product specificity is determined by the background physiology of each chassis strain. For example, the ratio of functional Esm1 to Esm2 might be important, as discussed previously (Ahuja et al., 2008; Xu et al., 2013; Rui et al., 2012). For PDC BGCs 1–3, the PDC/PCA production ratio was much higher than for PDC BGC4. PDC/PCA ratios of up to 7.4, 6.9, and 9.0 occurred for PDC BGCs 1–3, respectively (Figure 5A–C). For chassis strains that could not produce PDC well (EC01, AM04, and EB09), the PDC/PCA ratios were much smaller, even with expression of BGCs 1–3. Perhaps PhzG homologs were not functioning well in these particular chassis strains. Among the chassis strains, XP01 showed the highest selectivity for PDC production over PCA production.

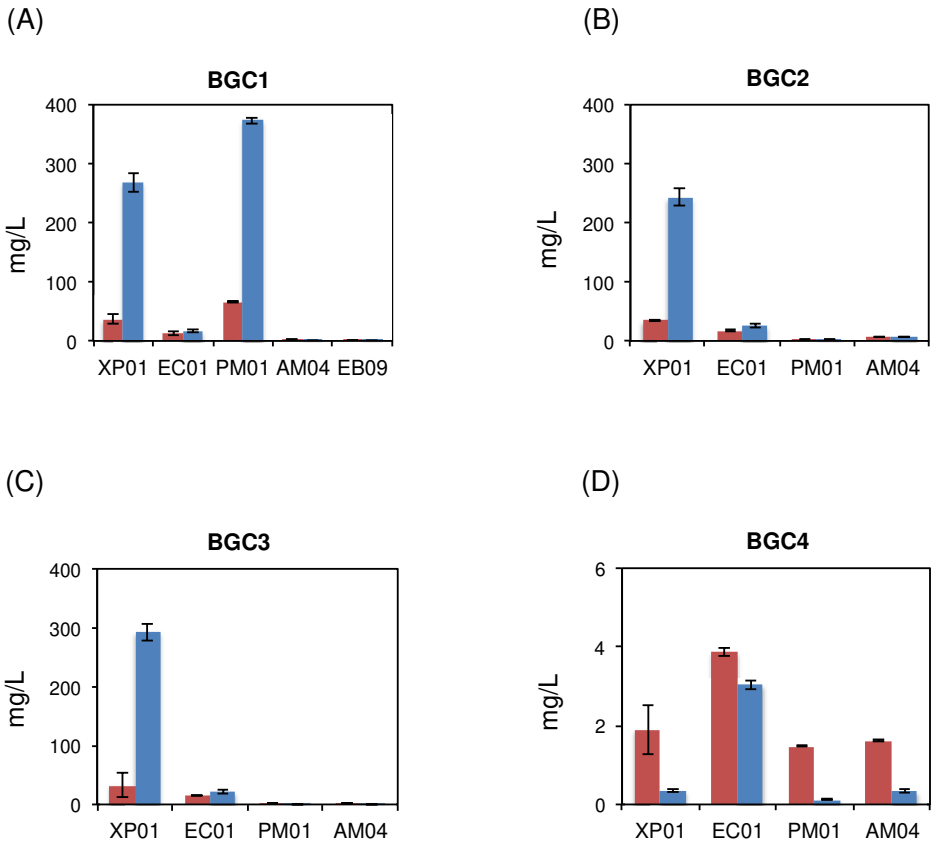

Figure 5. PCA and PDC production from strains expressing PDC BGCs. Heterologous PCA (red) and PDC (blue) production from the four PDC BGCs (A–D) in selected chassis strains. Error bars represent s.d.; n = 3 technically independent experiments.

3.5. Investigation of crosstalk between heterologously expressed Phz pathways and native pathways in each chassis strain

Because some XP species are also known to produce diverse Phz derivatives (Shi et al., 2019), we investigated whether the heterologously expressed Phz pathways interact with native pathways in each chassis strain. The XP strains are entomopathogens, and many of their secondary metabolite BGCs are activated when they are infected with insects or insect larvae. Therefore, we tested Phz production using both M9 and larvae as media. With untargeted LC-HRMS metabolite analyses of the PCA and PDC recombinants, we visually inspected and identified potential Phz derivatives from the culture extracts of specific chassis strains with the same UV absorbance as PCA and PDC standards, 228

and 372 nm, respectively. The *p*-values between the target and corresponding control groups for peak height were smaller than 0.005. These compounds showed mass-to-charge ratios identical to those of predicted structures **1**–**6**, as well as reasonable MS/MS fragmentation fingerprints (Supplementary Figure 1S, Figure 2S), some of which are uncharacterized compounds with no available MS/MS data for comparison. We speculate that these Phz derivatives are generated via hydroxylation or methoxylation on the aromatic ring, N-methylation, or amidation on the carboxyl group, possibly functioning by chassis-customized oxidases, methyltransferase, or aminotransferase. We also identified one Phz derivative that is likely a pelagiomicin derivative previously not reported. Further purification and structural identification for those metabolites is in process.

4. Discussion

4.1. This multi-chassis approach enabled identification of potent producers of both PCA and PDC

Most metabolic engineering efforts have focused on improving product yield by generating a number of different pathway variants to express in single host organisms (Jin et al., 2015; Cambray et al., 2018). We, as well as other researchers, have previously reported that expression of the same pathways in chassis strains even of different subspecies can dramatically alter pathway performance (Martinez et al., 2004; Wang et al., 2019). We interpret this to mean that heterologous BGC expression can be significantly influenced by the host's specific regulatory elements, including transcription, translation, post-translational modification, and folding. Additional relevant factors are availability of substrates and co-factors and the host's tolerance of products and their intermediates. However, the ability to screen and identify suitable host strains for formation of desired products has been limited by lack of versatile genetic tools. Our group previously developed CRAGE as a versatile genome engineering technology to overcome this limitation. CRAGE delivers a large, complex payload as a single copy directly into the chromosome of non-model bacteria and enables parallel

expression of target pathways in diverse chassis strains across multiple species and phyla (Wang et al., 2019). This multi-chassis approach allows rapid identification of chassis strains suitable for producing desired products.

When we introduced PCA BGCs into the genomes of 23 chassis strains across multiple genera within γ-proteobacteria, PCA was produced by all recombinant strains. As expected, PCA production titer varied dramatically, by as much as 52 times from the lowest to the highest producers (Figure 3A). Strains *P. simiae* (PM01), *E. coli* (EC01), and *X. doucetiae* (XP01) were among the top producers, at 47, 63, and 131 mg/L, respectively. These production levels are comparable to those of native PCA producers with a few rounds of metabolic engineering modifications (Jin et al., 2015). Subsequent expression of partially refactored PDC BGCs 1–4 in these strains also identified XP01 and PM01 as strong PDC producers; they produced 293 and 373 mg/L of PDC, respectively. BGC4 was previously assembled by Rui et al. (2012), heterologously expressed in *E. coli*. PDC production from this strain was, however, very limited (6.7 mg/L), an amount comparable to our EC01_BGC4 result (Figure 5D). Using bioinformatics analyses, we identified three additional candidate genes for PDC synthesis. The pathways built based on these genes (PDC BGCs 1–3) enhanced PDC production. Interestingly, all three of these BGCs produced high levels of PDC in XP01, while only BGC1 produced high levels of PDC in PM01. Because PhzC–F were confirmed active in all strains, either PhzA/B, PhzG, or both were likely prematurely produced in many strains. XP01 may have a molecular chaperon or physiological properties that are more suitable for maturation of these enzymes than do the other chassis strains. Notably, both XP01 and PM01 expressing PDC BGCs can serve as potent strains for PDC production, as well as platform strains for function characterization of BGCs for Phz derivatives. Combining the CRAGE-CRISPR systems (Ke et al., 2021; Liu et al., 2020), we can further optimize heterologous production of both PCA and PDC.

4.2. The PDC/PCA production ratio is dramatically different in different species

Many BGCs produce several metabolites. Some of them are simply intermediates of the final products (Ziegler and Facchini, 2008; Shi et al., 2019), while others are structurally similar to the final products produced from promiscuous enzyme activity (Li et al., 2010; Chevrette et al., 2020). These BGC properties are important, as they can expand the secondary metabolome and thereby make the producing microbes better fit to survive in a new environment. In the case of PDC BGC expression, we identified PCA as the major byproduct. Different chassis strains showed different selectivity for PDC versus PCA production. Specifically, the PDC/PCA ratio of XP01_BGCs1–3 was up to 9, while the ratios for *E. coli* (EC01)_BGCs1–3 and PM01_BGC1 were around 2 and 6, respectively. PDC production from BGC4 was less than PCA production in XP01, EC01, PM01, and AM04; these PDC/PCA ratios ranged from 0.08 to 0.8. This shows that combinatorial expression of different PDC BGCs and the multi-chassis approach were able to shift PDC/PCA production over 100-fold.

Among the steps of core Phz biosynthesis, DHHA is the last stable intermediate in the pathway leading to PCA and PDC. It is isomerized into 6-amino-5-oxocyclohex-2-ene-1-carboxylic acid (AOCHC) by PhzF (Figure 1) (Blankenfeldt et al., 2004; Parsons et al., 2004b; Blankenfeldt and Parsons, 2014). Then the highly reactive AOCHC spontaneously undergoes a twofold self-condensation aided by PhzF (Blankenfeldt et al., 2004) and/or PhzA/B (Ahuja et al., 2008) to form hexahydrophenazine-1,6-dicarboxylic acid (HHPDC). HHPDC is not stable and undergoes rapid uncatalyzed decarboxylation to tetrahydrophenazine-1,6-carboxylic acid (THPCA), which explains why PCA is always observed as a major byproduct of PDC biosynthesis (Parsons et al., 2004b). Then PhzG acts on THPCA or directly on HHPDC, thereby contributing to the generation of both PCA and PDC, respectively. The varied ratio of PDC to PCA production during heterologous PDC synthesis by different host microbes therefore stems from different relative activities of the PhzF, PhzA/B dimer, and

PhzG enzymes, and also from the availability of oxygen (Rui et al., 2012). Moreover, the specificity of PhzA/B and PhzG activity alters depending on the background physiology of host organisms, suggesting that PhzG might have been formed more maturely in XP01 than in the other strains, and as a result it produced significantly more PDC than PCA, whereas *E. coli* (EC01) produced a premature form of PhzG and almost equal amounts of PDC and PCA.

4.3. Crosstalk between heterologous pathways and internal pathways in each chassis could generate new products

During bacterial evolution, BGC integration via lateral gene transfer is thought to be beneficial because it produces genetic variation that can drive metabolic adaptation potential and offer opportunities to rapidly test cell fitness for tolerating the produced metabolites (Ziemert et al., 2014; Milner et al., 2019). Secondary metabolic pathways are typically more diversity-oriented than target-oriented compared with biosynthesis in primary metabolic pathways (Fischbach and Clardy, 2007). From an evolutionary standpoint, this suggests that introduction of a heterologous metabolic pathway may result in a variety of adaptations in the metabolic and regulatory networks, as well as in enzymes in the pathway itself (Kim and Copley, 2012). One of the major functional consequences is crosstalk between heterologous pathways and internal pathways of the chassis host, which can alter the gene repertoire and produce functional molecule(s) to justify the existence of new BGCs, thereby improving cell fitness (Gutin et al., 2015) and thus enabling diversification of the secondary metabolome during biosynthesis (Wang et al., 2019; Shi et al., 2019). This implies that using a multi-chassis approach for BGC expression may result in production of hosts specifically tailored for producing specific secondary metabolites, and in expansion of the secondary metabolome as a population (Wang et al., 2019).

Potential Phz derivatives from the PCA and PDC recombinants were detected in specific chassis strains by untargeted LC-HRMS-based metabolite analyses (Supplementary Figure 1S). These newly produced Phz derivatives possess functionalities beyond those of the core Phz structure and may have agricultural

and/or therapeutic potential. Both XP01 and PM01 are known to be potential secondary metabolite producers. Diverse physiological backgrounds expressing the same BGCs may result in increased diversity of secondary metabolite structures. Our CRAGE-facilitated multi-chassis approach can be applied to other natural-product BGCs, which may lead to development of novel bioactive compounds for various clinical or agricultural applications. Continued technological and conceptual advances in strain engineering and genetic techniques will open up opportunities to fully explore and harness the immensely diverse chemical repertoires of Nature.

5. Conclusion

We showed here that PCA and PDC can be produced using a multi-chassis approach facilitated by CRAGE. Evaluation and optimization of Phz BGC expression hosts with various genetic backgrounds enhanced yield of the core Phzs PCA and PDC. Detection of potential Phz derivatives offers a set of strains favorable for characterization of Phz-modifying enzymes. This work indicates the potential for *X. doucetiae* (XP01) and *P. simiae* WCS417 (PM01) to optimize PCA and PDC production, and their usefulness as platform strains for functional characterization of Phz BGCs.

Acknowledgements

This work was conducted by the US Department of Energy's Joint Genome Institute, a DOE Office of Science User Facility, operated by Lawrence Berkeley National Laboratory under Contract no. DE-AC02-05CH11231. We thank Dr. Satoshi Yuzawa (Joint BioEnergy Institute) for the *E. coli* BL21_DE3 sfp strain. We thank Dr. Linda Thomashow (Washington State University) for the *Pseudomonas fluorescens* Q8R1 strain and the *E. coli* strain with the pT7_6A-G plasmid. We thank Ben Cole (Joint Genome Institute) for the *Pseudomonas*

fluorescens WCS417r strain. We thank Zhe Rui (Louisiana State University) for the *E. coli* DH5a strain harboring the pZR28_EsmA1A2 plasmid. We thank Anita Wahler for professional editing.

Declaration of Interest

Lawrence Berkeley National Laboratory filed a United States patent application for CRAGE technology (US patent 20190048354). The patent is currently pending. The application lists Yasuo Yoshikuni, Zhiying Zhao, and Cameron Coates as inventors.

References

Abraham A, Philip S, Jacob MK, Narayanan SP, Jacob CK, Kochupurackal J, 2015. Phenazine-1-carboxylic acid mediated anti-oomycete activity of the endophytic *Alcaligenes* sp. EIL-2 against *Phytophthora meadii*. Microbiol Res, 170, 229–234.

Ahuja EG, Janning P, Mentel M, Graebsch A, Breinbauer R, Hiller W, Costisella B, Thomashow LS, Mavrodi DV, Blankenfeldt W, 2008. PhzA/B catalyzes the formation of the tricycle in phenazine biosynthesis. J Am Chem Soc, 130, 17053–17061.

Baron SS, Terranova G, Rowe JJ, 1989. Molecular mechanism of the antimicrobial action of pyocyanin. Curr Microbiol, 18, 223–230.

Bauman KD, Li J, Murata K, Mantovani SM, Dahesh S, Nizet V, Luhavaya H, Moore BS, 2019. Refactoring the cryptic streptophenazine biosynthetic gene cluster unites phenazine, polyketide, and nonribosomal peptide biochemistry. Cell Chem Biol, 26, 724–736.

Blankenfeldt W, 2013. The Biosynthesis of Phenazines. In Microbial Phenazines; Chincholkar S, Thomashow L, Eds; Springer: Heidelberg, Berlin, Germany; Chapter 1, pp 1–17.

Blankenfeldt W, Kuzin AP, Skarina T, Korniyenko Y, Tong L, Bayer P, Janning P, Thomashow LS, Mavrodi DV, 2004. Structure and function of the

phenazine biosynthesis protein PhzF from *Pseudomonas fluorescens.* Proc Natl Acad Sci USA, 101, 16431–16436.

Blankenfeldt W, Parsons JF, 2014. The structural biology of phenazine biosynthesis. Curr Opin Struct Biol, 29, 26–33.

Blin K, Medema MH, Kazempour D, Fischbach MA, Breitling R, Takano E, Weber T. 2013. antiSMASH 2.0: a versatile platform for genome mining of secondary metabolite producers. Nucleic Acids Res, 41, W204–W212.

Cambray G, Guimaraes JC, Arkin AP, 2018. Evaluation of 244,000 synthetic sequences reveals design principles to optimize translation in *Escherichia coli*. Nat Biotechnol, 36, 1005–1015.

Chevrette MG, Gutiérrez-García K, Selem-Mojica N, Aguilar-Martínez C, Yañez-Olvera A, Ramos-Aboites HE, Hoskisson PA, Barona-Gómez F, 2020. Evolutionary dynamics of natural product biosynthesis in bacteria. Nat Prod Rep, 37, 566–599.

Cimermancic P, Medema MH, Claesen J, Kurita K, Wieland Brown LC, Mavrommatis K, Pati A, Godfrey PA, Koehrsen M, Clardy J, Birren BW, Takano E, Sali A, Linington RG, Fischbach MA. 2014. Insights into secondary metabolism from a global analysis of prokaryotic biosynthetic gene clusters. Cell, 158, 412–421.

Coates RC, Bowen BP, Oberortner E, Thomashow L, Hadjithomas M, Zhao Z, et al., 2018. An integrated workflow for phenazine-modifying enzyme characterization. J Ind Microbiol Biotechnol, 45, 567–577.

Dasgupta D, Kumar A, Mukhopadhyay B, Sengupta TK, 2015. Isolation of phenazine 1,6-di-carboxylic acid from *Pseudomonas aeruginosa* strain HRW.1-S3 and its role in biofilm-mediated crude oil degradation and cytotoxicity against bacterial and cancer cells. Appl Microbiol Biotechnol, 99, 8653–8665.

Fischbach MA, Clardy J, 2007. One pathway, many products. Nat Chem Biol, 3, 353–355.

Geiger A, Keller-Schierlein W, Brandl M, Zähner H, 1988. Metabolites of microorganisms. 247. Phenazines from *Streptomyces antibioticus*, strain Tü 2706. J Antibiot, 41, 1542–1551.

Gibson GG, Young L, Chuang RY, Venter JC, Hutchison CA III, Smith HO, 2009. Enzymatic assembly of DNA molecules up to several hundred kilobases. Nat Methods, 6, 343–345.

Giddens SR, Feng Y, Mahanty HK, 2002. Characterization of a novel phenazine antibiotic gene cluster in *Erwinia herbicola* Eh1087. Mol Microbiol, 45, 769–783.

Gross H, Loper JE, 2009. Genomics of secondary metabolite production by Pseudomonas spp. Nat Prod Rep, 26, 1408-1446.

Guo S, Wang Y, Dai B, Wang W, Hu H, Huang X, Zhang X, 2017. *PhzA*, the shunt switch of phenazine-1,6-dicarboxylic acid biosynthesis in *Pseudomonas chlororaphis* HT66. Biotechnol Prod Bioprocess Eng, 101, 7165–7175.

Guo S, Wang Y, Bilal M, Hu H, Wang W, Zhang X, 2020. Microbial synthesis of antibacterial phenazine-1,6-dicarboxylic acid and the role of PhzG in *Pseudomonas chlororaphis* GP72AN. J Agric Food Chem, 68, 2373–2380.

Gutin J, Sadeh A, Rahat A, Aharoni A, Friedman N, 2015. Condition-specific genetic interaction maps reveal crosstalk between the cAMP/PKA and the HOG MAPK pathways in the activation of the general stress response. Mol Syst Biol, 11, 829–849.

Guttenberger N, Blankenfeldt W, Breinbauer R, 2017. Recent developments in the isolation, biological function, biosynthesis, and synthesis of phenazine natural products. Bioorg Med Chem, 25, 6149–6166.

Hadjithomas M, Chen IMA, Chu K, Ratner A, Palaniappan K, Szeto E, et al., 2015. IMG-ABC: a knowledge base to fuel discovery of biosynthetic gene clusters and novel secondary metabolites. MBio, 6, e00932-15.

Hernandez ME, Kappler A, Newman DK, 2004. Phenazines and other redox-active antibiotics promote microbial mineral reduction. Appl Environ Microbiol, 70, 921–928.

Imamura N, Nighijima M, Takedera T, Adachi K, Sakai M, Sano H, 1997. New anticancer antibiotics pelagiomicins, produced by a new marine bacterium *Pelagiobacter variabilis*. J Antibiot. 50, 8–12.

Jin K, Zhou L, Jiang H, Sun S, Fang Y, Liu J, Zhang X, He Y, 2015. Engineering the central biosynthetic and secondary metabolic pathways of *Pseudomonas aeruginosa* strain PA1201 to improve phenazine-1-carboxylic acid production. Metab Eng, 32, 30–38.

Johnson LE, Dietz A, 1969. Lomofungin, a new antibiotic produced by *Streptomyces lomondensis* sp. n. Appl Microbiol, 17, 755–759.

Ke J, Yoshikuni Y, 2020. Multi-chassis engineering for heterologous production of microbial natural products. Curr Opin Biotech, 62, 88–97.

Ke J, Robinson D, Wu ZY, Kuftin A, Louie K, Kosina S, et al., 2021. CRAGE-CRISPR facilitates rapid activation of secondary metabolite biosynthetic gene clusters in bacteria. Cell Chem Biol, In press. doi.org/10.1016/j.chembiol.2021.08.009.

Khan SR, Mavrodi DV, Jog GJ, Suga H, Thomashow LS, Farrand SK, 2005. Activation of the phz operon of *Pseudomonas fluorescens* 2-79 requires the LuxR homolog PhzR, *N*-(3-OH-Hexanoyl)-L-homoserine lactone produced by the LuxI homolog PhzI, and a *cis*-acting *phz* box. J Bacteriol, 18, 6517 –27.

Kim J, Copley SD, 2012. Inhibitory cross-talk upon introduction of a new metabolic pathway into an existing metabolic network. Proc Natl Acad Sci USA, 109, E2856-E2864.

Kunakom S, Eustáquio AS, 2019. Natural products and synthetic biology: where we are and where we need to go. mSystems, 4:e00113–19.

Laursen JB, Nielsen J, 2004. Phenazine natural products: biosynthesis, synthetic analogues, and biological activity. Chem Rev, 104, 1663–1686.

Li B, Sher D, Kelly L, Shi Y, Huang K, Knerr PJ, Joewono I, Rusch D, Chisholm SW, van der Donk WA, 2010. Catalytic promiscuity in the biosynthesis of cyclic peptide secondary metabolites in planktonic marine cyanobacteria. Proc Natl Acad Sci USA, 107, 10430–10435.

Liu H, Robinson DS, Wu ZY, Kuo R, Yoshikuni Y, Blaby IK, et al., 2020. Bacterial genome editing by coupling Cre-lox and CRISPR-Cas9 systems. PLoS One, 15, e0241867.

Markowitz VM, Chen IM, Chu K, Szeto E, Palaniappan K, Pillay M, Ratner A, Huang J, Pagani I, Tringe S, Huntemann M, Billis K, Varghese N, Tennessen K, Mavromatis K, Pati A, Ivanova NN, Kyrpides NC. 2014a. IMG/M 4 version of the integrated metagenome comparative analysis system. Nucleic Acids Res, 42, D568–D573.

Markowitz VM, Chen IM, Palaniappan K, Chu K, Szeto E, Pillay M, Ratner A, Huang J, Woyke T, Huntemann M, Anderson I, Billis K, Varghese N, Mavromatis K, Pati A, Ivanova NN, Kyrpides NC. 2014b. IMG 4 version of the integrated microbial genomes comparative analysis system. Nucleic Acids Res, 42, D560–D567.

Martinez A, Kolvek SJ, Yip CLT, Hopke J, Brown KA, MacNeil IA, Osburne MS, 2004. Genetically modified bacterial strains and novel bacterial artificial chromosome shuttle vectors for constructing environmental libraries and detecting heterologous natural products in multiple expression hosts. Appl Environ Microbiol, 70, 2452–2463.

Mavrodi DV, Ksenzenko VN, Bonsall RF, Cook RJ, Boronin AM, Thomashow LS, 1998. A seven-gene locus for synthesis of phenazine-1- carboxylic acid by *Pseudomonas fluorescens* 2-79. J Bacteriol 180, 2541–2548.

Mavrodi DV, Peever TL, Mavrodi OV, Parejko JA, Raaijmakers JM, Lemanceau P, et al., 2010. Diversity and evolution of the phenazine biosynthesis pathway. Appl Environ Microbiol, 76, 866–879.

McDonald M, Mavrodi DV, Thomashow LS, Floss HG, 2001. Phenazine biosynthesis in *Pseudomonas fluorescens*: branchpoint from the primary shikimate biosynthetic pathway and role of phenazine-1,6-dicarboxylic acid. J Am Chem Soc, 123, 9459–9460.

Mentel M, Ahuja EG, Mavrodi DV, Breinbauer R, Thomashow LS, Blankenfeldt W, 2009. Of two make one: the biosynthesis of phenazines. Chembiochem, 10, 2295–2304.

Milner DS, Attah V, Cook E, Maguire F, Savory FR, Morrison M, Müller CA, Foster PG, Talbot NJ, Leonard G, Richards TA, 2019. Environment-dependent fitness gains can be driven by horizontal gene transfer of transporter-encoding genes. Proc Natl Acad Sci USA, 116, 5613–5622.

Myhren LE, Nygaard G, Gausdal G, Sletta H, Teigen K, Degnes KF, Zahlsen K, Brunsvik A, Bruserud Ø, Døskeland SO, Selheim F, Herfindal L, 2013. Iodinin (1,6-Dihydroxyphenazine 5,10-Dioxide) from *Streptosporangium* sp. induces apoptosis selectively in Myeloid Leukemia cell lines and patient cells. Mar Drugs, 11, 332–349.

Oberortner E, Cheng JF, Hillson NJ, Deutsch S, 2017. Streamlining the design-to-build transition with build-optimization software tools. ACS Synth Biol, 6, 485–496.

Parsons JF, Calabrese K, Eisenstein E, Ladner JE, 2003. Structure and mechanism of *Pseudomonas aeruginosa* PhzD, an isochorismatase from the phenazine biosynthetic pathway. Biochemistry, 42, 5684–5693.

Parsons JF, Calabrese K, Eisenstein E, Ladner JE. 2004a. Structure of the phenazine biosynthesis enzyme PhzG. Acta Crystallogr D Biol Crystallogr, 60, 2110–2113.

Parsons JF, Song F, Parsons L, Calabrese K, Eisenstein E, Ladner JE, 2004b. Structure and function of the phenazine biosynthesis protein PhzF from *Pseudomonas fluorescens* 2–79. Biochemistry, 43, 12427–12435.

Pierson LS, Pierson EA, 2010. Metabolism and function of phenazines in bacteria: impacts on the behavior of bacteria in the environment and biotechnological processes. Appl Environ Microbiol, 86, 1659–1670.

Podojil M, Gerber NN, 1967. The biosynthesis of 1,6-phenazinediol 5,10-dioxide (iodinin) by *Brevibacterium iodinum*. Biochemistry, 6, 2701-2705.Rui Z, Ye M, Wang S, Fujikawa K, Akerele B, Aung M, et al., 2012. Insights into a divergent phenazine biosynthetic pathway governed by a plasmid-born Esmeraldin gene cluster. Chem Biol, 19, 1116–1125.

Schneemann I, Wiese J, Kunz AL, Imhoff JF, 2011. Genetic approach for the fast discovery of phenazine producing bacteria. Mar Drugs, 9, 772–789.

Shi YM, Brachmann AO, Westphalen MA, Neubacher N, Tobias NJ, Bode HB, 2019. Dual phenazine gene clusters enable diversification during biosynthesis. Nat Chem Biol, 15, 331–339.

Smanski MJ, Zhou H, Claesen J, Shen B, Fischbach MA, Voigt CA, 2016. Synthetic biology to access and expand nature's chemical diversity. Nat Rev Microbiol, 14, 135–149.

Wang B, Zhao Z, Jabusch LK, Chiniquy DM, Ono K, Conway JM, et al., 2020. CRAGE-duet facilitates modular assembly of biological systems for studying plant–microbe interactions. ACS Synth Biol, 2020, 9, 2610–2615.

Wang G, Zhao Z, Ke J, Engel Y, Shi YM, Zhang Z, et al., 2019. Chassis-independent recombinase-assisted genome engineering enables rapid activation of biosynthetic gene clusters. *Nat Microbiol*, 4, 2498–2510.

Xu N, Ahuja EG, Janning P, Mavrodi DV, Thomashow LS, Blankenfeldt W, 2013. Trapped intermediates in crystals of the FMN-dependent oxidase PhzG provide insight into the final steps of phenazine biosynthesis. Acta Crystallogr D Biol Crystallogr, 69, 1403–1413.

Zhang C, Sheng C, Wang W, Hu H, Peng H, Zhang X, 2015. Identification of the lomofungin biosynthesis gene cluster and associated flavin-dependent monooxygenase gene in *Streptomyces lomondensis* S01. PLoS One, 10, e0136228/1-e0136228.

Zhang MM, Wang Y, Ang EL, Zhao H, 2016. Engineering microbial hosts for production of bacterial natural products. Nat Prod Rep, 33(8), 963–987.

Zhao YY, Qian GL, Ye YH, Wright S, Chen H, Shen YM, Liu FQ, LC D, 2016. Heterocyclic aromatic N-oxidation in the biosynthesis of phenazine antibiotics from *Lysobacter antibioticus*. Org Lett, 18, 2495–2498.

Ziegler J, Facchini PJ, 2008. Alkaloid biosynthesis: metabolism and trafficking. Annu Rev Plant Biol, 59, 735–769.